Ultrabroadband chirped pulse second-harmonic spectroscopy: measuring the frequency-dependent second-order response of different metal films

Bernd Metzger,* Lili Gui, and Harald Giessen

4th Physics Institute and Research Center SCoPE, University of Stuttgart, 70569 Stuttgart, Germany
**Corresponding author: b.metzger@physik.uni-stuttgart.de*

Received July 15, 2014; revised August 5, 2014; accepted August 5, 2014;
posted August 8, 2014 (Doc. ID 217035); published September 4, 2014

We introduce a spectroscopic method for measuring the frequency-dependent second-order response using ultrabroadband strongly chirped laser pulses. The dispersion suppresses nonlinear frequency mixing, hence the second-order response of a material can be unambiguously retrieved. We demonstrate this method by measuring the frequency-dependent second-harmonic (SH) response of the metals gold, aluminium, silver, and copper in the wavelength range of about 900–1150 nm and compare the results to classical SH spectroscopy. The SH spectra indicate that interband transitions in the metals influence the overall nonlinear optical response.

OCIS codes: (190.2620) Harmonic generation and mixing; (190.4350) Nonlinear optics at surfaces; (260.3910) Metal optics; (300.6420) Spectroscopy, nonlinear.
http://dx.doi.org/10.1364/OL.39.005293

One of the key technologies in optics and photonics is white-light spectroscopy. It allows measuring the linear optical response of a sample over a broad spectral range. Beyond optical information, the linear optical spectra allow for drawing conclusions on the structural composition of the sample under investigation, e.g., when using circular dichroism spectroscopy [1]. In addition, nonlinear optical spectroscopy, which originates from intense light–matter interaction, has proven to deliver additional information. Second-harmonic (SH) generation spectroscopy, for example, enables studying the crystal structure of a noninversion symmetric medium [2–4]. Furthermore, SH imaging microscopy can in some cases give superb contrast when compared to ordinary optical microscopy [5–7].

In contrast to linear optical spectroscopy with a broadband light source, SH spectroscopy often uses a narrowband laser, and hence, the second-order response is measured only over a narrow frequency range. However, just like the linear optical response, which is governed by the first-order susceptibility $\chi^{(1)}(\omega)$, also the second-order susceptibility $\chi^{(2)}(\omega)$ in general is a frequency-dependent quantity, in particular, if the material exhibits linear optical resonances in the spectral range of interest [8]. Hence, it is desirable to have access to spectrally resolved values of the second-order susceptibility. In principle, ultrabroadband laser sources, which exhibit ultrashort pulse durations in the visible and the near infrared, are available and deliver the bandwidth and the light intensities, which should allow for measuring the second-order response over a broad spectral range [9–12]. However, the retrieval of the frequency-dependent second-order susceptibility $\chi^{(2)}(\omega)$ is rendered highly ambiguous when an ultrabroadband laser source is focused on the sample due to frequency mixing, as explained in the following.

Imagine for simplicity a laser source consisting of three different equally spaced frequency components overlapping in time as shown in Fig. 1(a). When focused onto a second-order nonlinear material, SH and sum-frequency (SF) generation can be observed, which results in a nonlinear spectrum that exhibits five distinct intensity peaks. In particular, the central peak in the nonlinear spectrum is composed of the SH signal of the fundamental frequency ω_2 as well as of the SF signal of the fundamental frequencies ω_1 and ω_3. For an unknown frequency-dependent second-order susceptibility it is impossible to determine the intensity ratio of both contributing effects to this central peak, which also renders the retrieval of the second-order susceptibility at the frequency ω_2 impossible.

Instead of ultrabroadband laser sources researchers therefore have implemented widely tunable narrowband lasers in order to avoid the SF mixing processes and to unambiguously measure the nonlinear response over a broad spectral range [13–16]. However, tunable systems often require a highly complex setup and suffer from power variations and instabilities, which make these experiments quite sophisticated and time consuming.

In this Letter, we introduce a new method for measuring an entire nonlinear SH spectrum using a single

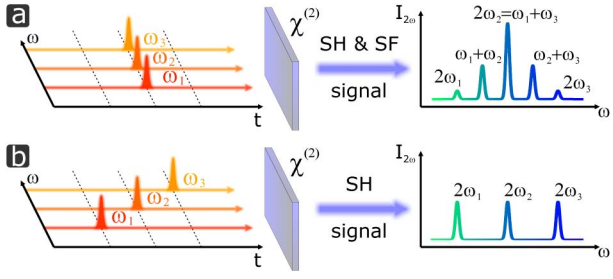

Fig. 1. Schematic illustration for second-harmonic (SH) and sum-frequency (SF) generation for three different incoming frequencies traveling (a) at zero time delay or (b) consecutively in time.

chirped broadband laser source. By introducing a large amount of dispersion we suppress SF mixing processes, since the different frequency components lack temporal overlap. Therefore, neighboring frequencies perform SH generation only individually, which is schematically depicted in Fig. 1(b). We demonstrate this method by measuring the optical SH response of various metal films in the wavelength range of about 900–1150 nm.

In order to demonstrate this SH measurement technique, which we term ultrabroadband chirped pulse (UCP) SH spectroscopy, we utilize a setup capable of producing ultrabroadband strongly chirped laser pulses as well as more narrowband tunable ultrashort laser pulses. Thereby, we are able to directly compare UCP and classical SH spectroscopy, where a narrowband laser is shifted step-wise in wavelength in order to measure a SH spectrum. The experimental setup is schematically depicted in Fig. 2(a). We use a homebuilt high-power Yb:KGW solitary mode-locked oscillator at a repetition rate of about 44 MHz, emitting 175 fs laser pulses with an average power of about 2.4 W and a central wavelength of 1027 nm [17]. These pulses are coupled into a large-mode area (LMA) photonic crystal fiber (PCF) for spectral broadening mainly by self-phase modulation. Subsequently, the laser pulses are sent into a prism sequence, which allows to compress the laser pulses down to a pulse duration of about 20 fs [18]. Furthermore, for amplitude and phase modulation we propagate the laser pulses through a 4f pulse shaper (PS), which includes a dual-mask liquid crystal spatial-light modulator [19]. Figure 2(b) shows a measured laser spectrum $I(\omega)$ at the output of the pulse shaper. For classical SH spectroscopy amplitude shaping using the spatial light modulator is utilized to generate narrowband Fourier-limited Gaussian-like 30 fs laser pulses tunable from 900 to 1150 nm [20]. In the case of UCP-SH spectroscopy we use the 4f setup in order to generate a group-delay dispersion (GDD) ϕ_2 of up to 5365 fs^2. The GDD ϕ_2 is defined by the second-derivative of the spectral phase $\phi(\omega)$ as $\phi_2 = \partial^2\phi(\omega)/\partial\omega^2$ [21].

Figure 2(c) shows a measured cross-correlation frequency-resolved optical gating (XFROG) trace of the ultrabroadband strongly chirped laser pulses, which

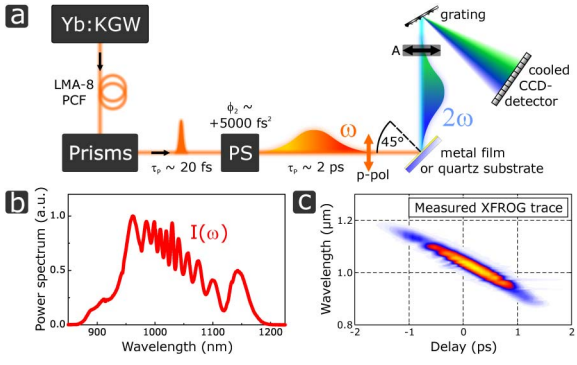

Fig. 2. (a) Experimental setup for ultrabroadband chirped pulse SH spectroscopy (LMA, large mode area; PCF, photonic crystal fiber; PS, pulse shaper; A, analyzer). (b) Measured laser spectrum at the output of the pulse shaper. (c) Measured XFROG trace of the ultrabroadband strongly chirped laser pulses.

we obtained via a SH cross-correlation with the Yb:KGW oscillator pulses [22]. Due to the large dispersion value ($\phi_2 = 5365$ fs^2) the laser pulses exhibit a pulse duration on the order of 2 ps. In particular, the different frequency components travel consecutively in time, which leads to the aforementioned suppression of SF mixing.

Finally, the output of the pulse shaper is focused by a 75 mm focal length achromatic lens on a sample surface, with an angle of incidence of 45° in p-polarization. The generated SH in reflection is recollimated by a fused silica lens, analyzed by a polarizer also oriented along p-polarization, and the SH signals are measured with a Peltier-cooled CCD camera attached to a spectrometer.

In order to show that SF mixing processes indeed become suppressed by introducing a large amount of dispersion we perform SH generation on a quartz crystal substrate in reflection with different values of GDD ϕ_2 and with the broadband laser spectrum shown in Fig. 2(b). The quartz crystal does not exhibit optical resonances in the spectral range of the fundamental laser light as well as the SH light. Hence we can assume a spectrally flat second-order susceptibility $\chi^{(2)}(\omega)$ [8]. For a flat second-order response the generated SH and SF signals are simply proportional to the complex electric field $E(t)$ of the laser pulses in the time domain squared [23]. In order to mathematically determine the SH spectrum $I^{(2)}(\omega)$ we have to perform a Fourier transform of the second-order electric-field amplitude $E^{(2)}(t) \propto E(t)^2$. Hence, in the frequency domain the SH spectrum $I^{(2)}(\omega)$ is given by a convolution:

$$I^{(2)}(\omega) \propto \left| \int_{-\infty}^{\infty} \mathrm{d}\omega' E(\omega') E(\omega - \omega') \right|^2. \qquad (1)$$

Here, $E(\omega) = |E(\omega)| \cdot e^{i\phi(\omega)}$ is the complex electric field of the laser pulses in the frequency domain. Measured

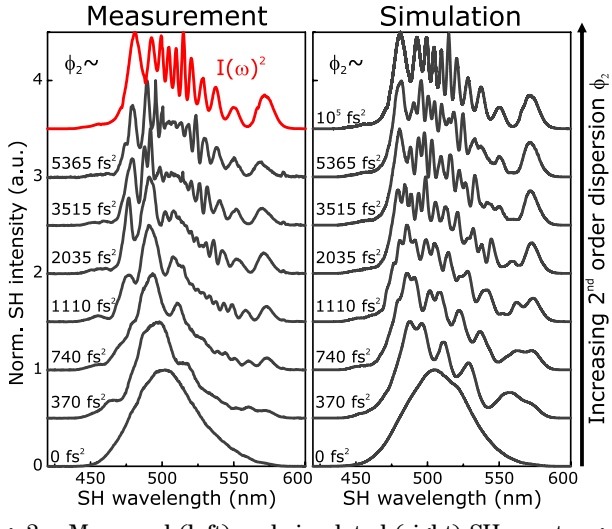

Fig. 3. Measured (left) and simulated (right) SH spectra generated on a quartz surface with the laser spectrum shown in Fig. 2(b) for different values of ϕ_2, increasing from bottom to top. The increase of dispersion suppresses SF mixing and as a result the SH spectra converge to the laser spectrum squared. The topmost red spectrum in the measurement column does not represent a SH spectrum, but corresponds to the measured laser spectrum from Fig. 2(b) squared, plotted over the SH wavelength for comparison.

and simulated SH spectra are depicted in Fig. 3 for increasing values of GDD ϕ_2 from bottom to top. For Fourier-limited laser pulses ($\phi_2 = 0$ fs^2) the SH spectrum constitutes a single broadband Gaussian-like intensity peak. Although our fundamental laser spectrum is strongly modulated, the SH spectrum exhibits a spectral Gaussian shape due to the SF mixing between all the frequency components. For increasing GDD in measurement and in simulation the SF generation becomes strongly suppressed. This means that as ϕ_2 increases the SH spectrum converges to the fundamental laser spectrum $I(\omega)$ squared. Then Eq. (1) simplifies to

$$\phi_2 \to \infty \Rightarrow I^{(2)}(2\omega) \propto I(\omega)^2 \propto |E(\omega)|^4. \tag{2}$$

The maximum value of GDD ϕ_2, which we are currently able to generate with the 4f setup, is about 5365 fs^2. Unfortunately, for this dispersion value SF mixing is not entirely suppressed yet but is strongly reduced. This circumstance slightly limits the spectral resolution of UCP-SH spectroscopy, which can be estimated from the phase difference $\Delta\phi = \frac{1}{2}\phi_2\Delta\omega^2$ between frequency components separated by $\Delta\omega$. If the phase difference $\Delta\phi$ between two frequencies approaches π these components interfere destructively and as a consequence SF generation will be suppressed. Using this condition the spectral resolution can be approximated by $\Delta\lambda = \lambda_0^2/\sqrt{2\pi c^2\phi_2}$, where λ_0 is the central wavelength and c is the speed of light. For $\lambda_0 = 1000$ nm and $\phi_2 = 5365$ fs^2 we obtain a value of about $\Delta\lambda \sim 18$ nm, which is sufficient for UCP-SH spectroscopy of metal films. When increasing the dispersion to even higher values the SH spectrum indeed converges to the laser spectrum $I(\omega)$ squared, which is shown in Fig. 3 in red for comparison.

In order to demonstrate UCP-SH spectroscopy and to measure the second-order response of metals over a broad spectral range we evaporated 100 nm thick films of gold, copper, silver, and aluminum on various quartz substrates by electron-beam evaporation. During the evaporation process a small area of the quartz surface was covered so that partially the surface of each quartz substrate remains blank. Subsequently, we measured the SH spectra of the metal films using the maximum available GDD of 5365 fs^2. Furthermore, the SH spectra from the metal films are divided by a SH spectrum generated at the interface of the blank quartz surface measured with the same maximum dispersion value. Therefore, we account for the spectral shape of the laser source and the influence of any wavelength-dependent components, very similar to linear optical white-light spectroscopy.

The experimental results of these measurements are depicted in Fig. 4. The blue data points correspond to the SH spectra measured via UCP-SH spectroscopy. These SH spectra exhibit quite high variance at the spectral positions where the reference SH signal from the quartz substrate is close to zero (see Fig. 3). Hence, for UCP-SH spectroscopy it is desirable to have an ultrabroadband laser spectrum available that is as smooth and flat as possible. As mentioned above, we also performed classical SH spectroscopy, shown in Fig. 4, by the red diamonds for comparison. Therefore, we utilized

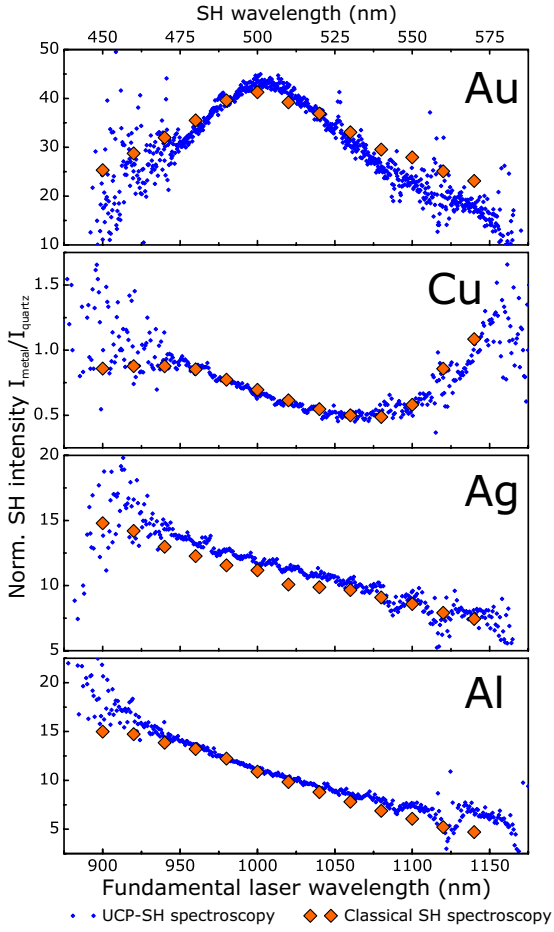

Fig. 4. SH spectroscopy of 100 nm thick bare-metal films plotted over the fundamental laser wavelength. The top axis shows the SH wavelength. The small blue data points are measured using UCP-SH spectroscopy. The red data points were obtained using classical SH spectroscopy.

narrowband Gaussian-shaped 30 fs laser pulses and tuned these over the entire spectral range in steps of 20 nm. For all SH spectra of the metal films we observe an excellent agreement between UCP and classical SH spectroscopy. In particular, in the SH response of the gold film we find a pronounced peak in the SH-generation efficiency close to a SH wavelength of about 500 nm. This peak in the SH spectrum of gold is most likely related to the onset of interband transitions, which occur for gold at around this spectral range [24]. For copper we observe a minimum in the SH spectrum at a SH wavelength of about 530 nm, but an increase toward longer wavelength. The excitation of interband transitions in copper sets is already slightly below 600 nm [25,26]. Therefore, the SH spectrum of copper indicates a peak at the long-wavelength side of the SH spectrum, however, our spectral range is too limited to entirely resolve this peak position. For silver and aluminum in our spectral window neither at the fundamental wavelength nor at the SH wavelength a resonance occurs. Hence, their SH response should be dominated by a free-electron nonlinearity, which is underlined by the fact that we observe very similar SH spectra for aluminum and silver in amplitude and spectral behavior. Furthermore, the SH spectra show a monotonic increase of the SH-generation efficiency toward

higher frequencies. These findings are consistent with previous studies of the SH response of metal films [13,14,27].

In conclusion, we introduced a spectroscopic SH measurement technique, called ultrabroadband chirped pulse (UCP) second-harmonic (SH) spectroscopy, for measuring the frequency-dependent SH response over a broad spectral range. We demonstrated this method by measuring the SH response of metal films in the near infrared from 900 to 1150 nm. We find the SH spectra of UCP and classical SH spectroscopy to be in excellent agreement. Interband transitions in the metals seem to influence the nonlinear optical SH spectra of the metal films. We believe that in the future UCP-SH spectroscopy might be implemented by propagating broadband ultrashort laser pulses through highly dispersive glasses, which could provide the required dispersion in a straightforward and simple fashion. Furthermore, UCP-SH spectroscopy might be utilized for measuring the spectrally resolved nonlinear response of semiconductors or plasmonic metamaterials, or for measuring the phase-matching bandwidth of nonlinear optical crystals for frequency conversion.

We gratefully acknowledge financial support from the Baden–Württemberg Stiftung (Kompetenznetz Funktionelle Nanostrukturen), the DFG (SPP1391, ultrafast nanooptics), the BMBF (13N10146), and the ERC (Complexplas). We thank M. Ubl for the evaporation of the metal films and S. De Zuani for the measurement of ellipsometric data of the metal films.

References

1. N. J. Greenfield, Nat. Protoc. **1**, 2876 (2007).
2. J. I. Dadap and T. F. Heinz, in *Encyclopedia of Modern Optics*, R. D. Guenther, D. G. Steel, and L. Bayvel, eds. (Elsevier, 2004), Vol. **5**, pp. 134–146.
3. R. V. Pisarev, J. Phys. C **5**, 8621 (1993).
4. V. V. Pavlov, R. V. Pisarev, A. Kirilyuk, and Th. Rasing, Phys. Rev. Lett **78**, 2004 (1997).
5. K. Klass, G. Mette, J. Güdde, M. Dürr, and U. Höfer, Phys. Rev. B **83**, 125116 (2011).
6. I. Freund, M. Deutsch, and A. Sprecher, Biophys. J. **50**, 693 (1986).
7. P. J. Campagnola and L. M. Loew, Nat. Biotechnol. **21**, 1356 (2003).
8. R. W. Boyd, *Nonlinear Optics* (Academic, 2008).
9. G. Krauss, S. Lohss, T. Hanke, A. Sell, S. Eggert, R. Huber, and A. Leitenstorfer, Nat. Photonics **4**, 33 (2010).
10. S. Rausch, T. Binhammer, A. Harth, J. Kim, R. Ell, F. X. Kärtner, and U. Morgner, Opt. Express **16**, 9739 (2008).
11. D. Brida, S. Bonora, C. Manzoni, M. Marangoni, P. Villoresi, S. De Silvestri, and G. Cerullo, Opt. Express **17**, 12510 (2009).
12. E. Goulielmakis, M. Schultze, M. Hofstetter, V. S. Yakovlev, J. Gagnon, M. Uiberacker, A. L. Aquila, E. M. Gullikson, D. T. Attwood, R. Kienberger, F. Krausz, and U. Kleineberg, Science **320**, 1614 (2008).
13. C. Matranga and P. Guyot-Sionnest, J. Chem. Phys. **115**, 9503 (2001).
14. E. K. L. Wong and G. L. Richmond, J. Chem. Phys. **99**, 5500 (1993).
15. S. Linden, F. B. P. Niesler, J. Förstner, Y. Grynko, T. Meier, and M. Wegener, Phys. Rev. Lett. **109**, 015502 (2012).
16. I. Sänger, D. R. Yakovlev, B. Kaminski, R. V. Pisarev, V. V. Pavlov, and M. Bayer, Phys. Rev. B **74**, 165208 (2006).
17. B. Metzger, A. Steinmann, F. Hoos, S. Pricking, and H. Giessen, Opt. Lett. **35**, 3961 (2010).
18. T. Südmeyer, F. Brunner, E. Innerhofer, R. Paschotta, K. Furusawa, J. C. Baggett, T. M. Monro, D. J. Richardson, and U. Keller, Opt. Lett. **28**, 1951 (2003).
19. A. M. Weiner, Rev. Sci. Instrum. **71**, 1929 (2000).
20. B. Metzger, A. Steinmann, and H. Giessen, Opt. Express **19**, 24354 (2011).
21. J.-C. Diels and W. Rudolph, *Ultrashort Laser Pulse Phenomena* (Academic, 2005).
22. S. Linden, H. Giessen, and J. Kuhl, Phys. Status Solidi B **206**, 119 (1998).
23. R. Trebino, *Frequency-Resolved Optical Gating: The Measurement of Ultrashort Laser Pulses* (Kluwer Academic, 2000).
24. R. L. Olmon, B. Slovick, T. W. Johnson, D. Shelton, S.-H. Oh, G. D. Boreman, and M. B. Raschke, Phys. Rev. B **86**, 235147 (2012).
25. P. B. Johnson and R. W. Christy, Phys. Rev. B **6**, 4370 (1972).
26. G. Petrocelli, S. Martellucci, and R. Francini, Appl. Phys. A **56**, 263 (1993).
27. C. M. Li, L. E. Urbach, and H. L. Dai, Phys. Rev. B **49**, 2104 (1994).